Imaging Agents

DOI: 10.1002/anie.201203190

Hydrogels Incorporating GdDOTA: Towards Highly Efficient Dual T_1/T_2 MRI Contrast Agents**

Thomas Courant, Valérie Gaëlle Roullin, Cyril Cadiou, Maïté Callewaert, Marie Christine Andry, Christophe Portefaix, Christine Hoeffel, Marie Christine de Goltstein, Marc Port, Sophie Laurent, Luce Vander Elst, Robert Muller, Michaël Molinari, and Françoise Chuburu**

Because of its sub-millimeter spatial resolution, the non-invasive nature of the examinations, and the absence of ionizing radiation, magnetic resonance imaging (MRI) is an important diagnostic imaging tool. However, this technique suffers from low detection sensitivity. To improve this aspect, millimolar concentrations of paramagnetic contrast agents (CAs) are often administered prior to examination, to enhance the image contrast and thus, to highlight pathological areas. The most commonly used CAs are gadolinium complexes (GdCAs).[1,2] GdCAs do not directly provide a signal, but they shorten the T_1 and/or T_2 relaxation times of water protons in the tissues.[1] Their efficiency is measured in terms of relaxivity r_1, which is defined as the relaxation rate enhancement of the water proton per millimolar metal ion. Until recently, all GdCAs were considered safe; unfortunately, it has been demonstrated that some of them may trigger the development of nephrogenic systemic fibrosis (NSF) in patients with renal failure.[3] Improvement is therefore needed to increase the relaxivity of known, low-risk GdCAs to decrease the injected doses. The interpretation of SBM theory[4] gives some guidelines on how to amplify r_1. For applications at 0.5–1.5 T, high relaxivity can be achieved by high payload of active magnetic centers, by controlling the tumbling motion of the GdCAs, and by ensuring optimal water residency times in the gadolinium coordination sphere.[5] In this challenging area, recent progress has been achieved with the integration of gadolinium chelates into nanoparticles. For this purpose, many nanoparticles have been developed (modified natural nanoparticles,[6] liposomal nanoparticles,[6] micelles,[6] metal–organic frameworks,[7] fullerenes,[8] inorganic nanoparticles[9]) but the predicted high relaxivities (on the order of 100 $mM^{-1}s^{-1}$) have rarely been obtained.[9c–e]

In this respect, our goal herein was to develop a new and straightforward synthesis of high-relaxivity gadolinium nanoparticles for MRI applications, with optimized nanoparticle production characteristics, gadolinium loading, and relaxivity at the same time. To take the risk of NSF disease into account, we choose to encapsulate a well-known, low-risk CA, $[GdDOTA]^-$ (DOTA = 1,4,7,10-tetraazacyclododecane-1,4,7,10-tetraacetic acid; the GdCA of DOTAREM). Because of its hydrophilic nature, the encapsulation of $[GdDOTA]^-$ was made in a hydrophilic polymer matrix. For biocompatibility reasons, chitosan (CH)[10] and hyaluronic acid (HA)[11] were chosen for the polymer matrix. CH is a positively charged, biocompatible polysaccharide composed of *N*-acetylglucosamine and glucosamine residues. HA is a natural, non-toxic, negatively charged polymer composed of glucuronic acid and *N*-acetylglucosamine residues. Herein, the

[*] Dr. T. Courant, Dr. V. G. Roullin, Dr. M. Callewaert, Prof. M. C. Andry
Institut de Chimie Moléculaire de Reims, CNRS UMR 7312,
Université de Reims Champagne Ardenne, UFR de Pharmacie
51 rue Cognacq-Jay, 51100 Reims (France)
E-mail: gaelle.roullin@univ-reims.fr

Dr. T. Courant, Dr. C. Cadiou, Prof. F. Chuburu
Institut de Chimie Moléculaire de Reims, CNRS UMR 7312,
Université de Reims Champagne Ardenne
BP 1039, 51687 Reims Cedex 2 (France)
E-mail: francoise.chuburu@univ-reims.fr

C. Portefaix, Prof. C. Hoeffel
Service de Radiologie, CHU de Reims-Hôpital Maison Blanche
51092 Reims Cedex (France)

M. C. de Goltstein, Dr. M. Port
GUERBET
BP57400, 95943 Roissy CdG Cedex (France)

Dr. S. Laurent, Prof. L. V. Elst, Prof. R. N. Muller
University of Mons, NMR & Molecular Imaging Laboratory,
Department of General Organic & Biomedical Chemistry 19 avenue Maistriau
7000 Mons (Belgium)

Prof. R. N. Muller
Center for Microscopy and Molecular Imaging
6041 Charleroi (Belgium)

Prof. M. Molinari
Laboratoire de Recherche en Nanosciences, EA4682 Université de Reims Champagne Ardenne
51685 Reims Cedex 2 (France)

[**] The work is supported by the Region Champagne Ardenne (T.C.), the DRRT Champagne Ardenne (MESR) and the EU-program FEDER (Project NanoBio2, Nano'Mat Platform). The ARC (research contract 00/05-258, 05/10-335, and AUWB-2010—10/15-UMONS-5), the FNRS, ENCITE program, the COST D38 (Metal-Based Systems for Molecular Imaging Applications), the European Network of Excellence EMIL (European Molecular Imaging Laboratories) program LSCH-2004-503569, and the Center for Microscopy and Molecular Imaging (CMMI, supported by the European Regional Development Fund and the Walloon Region) are thanked for their support. Dr. C. Kowandy and Dr. M. Pothecary are acknowledged for their help in polymer characterization. L. Wortham is thanked for her help in TEM-EDXS. L. Van Gulik, Dr. K. Plé and Prof. E. K. Brechin are warmly acknowledged for helpful discussions.

Supporting information for this article (experimental details) is available on the WWW under http://dx.doi.org/10.1002/anie.201203190.

synthesis and characterization of GdDOTA loaded nanoparticles, obtained by interaction of CH and HA, are reported. We demonstrate that $[GdDOTA]^-$ entrapped in the polymer nanomatrix has the tremendous advantage of being an efficient dual-mode T_1/T_2 contrast agent.

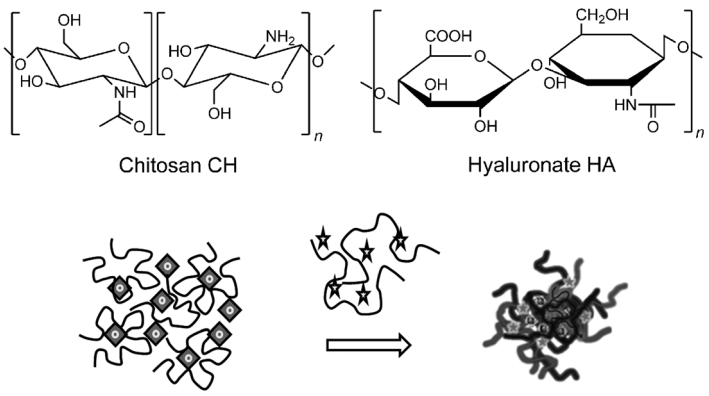

Scheme 1. Ionic-gelation process between chitosan, H[GdDOTA] (diamonds), hyaluronic acid, and TPP (stars).

The polysaccharide nanoparticles (NPs) were synthesized using an ionotropic gelation process[10,11] (Scheme 1) with low molecular weight CH and HA (Supporting Information, Table S1 and Figure S1). Typically, CH was solubilized in a citric acid solution and allowed to react with an aqueous mixture of sodium tripolyphosphate (TPP) and HA. The spontaneous formation of inter- and intramolecular electrostatic-mediated cross-links between polyanions and protonated CH chains provoked the gelation process.[12] The resulting NPs were then purified by dialysis and concentrated by tangential filtration.

Gadolinium-loaded NPs were prepared using the same procedure, by incorporating increasing amounts of H[GdDOTA] in the CH phase.[12] The resulting GdDOTA⊂NPs were subsequently purified as described above. The final colloidal suspension was stable for weeks at room temperature, owing to electrostatic repulsion. Both dynamic light scattering (DLS) analysis and AFM images (Figure 1 a,b) showed that the GdDOTA⊂NPs were narrowly monodispersed and spherical, with a mean diameter between 235 and 284 nm (Supporting Information, Table S2 and Figure S2). Moreover, the presence of Gd^{III} inside the NPs was verified by TEM-energy-dispersive x-ray spectroscopy (TEM-EDXS; Figure 1 c).

To check that no demetalation occurred under the acidic conditions of the synthesis, fluorescence spectra of $[Eu(DOTA)]^-$, which is isostructural to $[Gd(DOTA)]^-$, were recorded in a citric acid solution for three days (Supporting Information, Figure S3). The corresponding spectra did not evolve with time which is evidence that $[Eu(DOTA)]^-$, and thus $[GdDOTA]^-$, remained intact throughout the encapsulation process.

The inductively coupled plasma atomic-emission spectroscopy (ICP-AES) analysis of GdDOTA⊂NPs indicated that according to the initial Gd quantity, the Gd loading increased from 1.6% to 4.1%; increasing amounts of GdDOTA were incorporated in several distinct syntheses. After nanoparticle recovery and purification, the determination of Gd loadings indicated that the more GdDOTA initially incorporated, the more Gd complexes were trapped inside the nanoparticles (Supporting Information, DLE Equation (1) and Table S3; DLE = drug-loading efficiency) without drastic modifications of the NP production yield and morphology. This led to an average number of Gd chelates per NP in the range of $(0.79–3.41)\times10^5$ (Supporting Information). This high loading, which correlated with the existence of efficient hydrophilic interactions between the polymer matrix and entrapped chelates, was comparable to the loading of supramolecular assemblies between Gd chelates, dextran, and poly-β-cyclodextrin.[13]

To mimic the leakage of Gd from CAs under in vivo conditions, the release kinetics of the encapsulated $[GdDOTA]^-$ was evaluated in phosphate buffer at 37 °C under sink conditions (that is, 'sink conditions' is defined as the volume of medium at least greater than three times that required to form a saturated solution of a drug substance; see Supporting Information, Figure S4). In PBS buffer, no significant complex release was detected for three days. This behavior, typical of hydrogels,[14] is in strong contrast to the behavior of GdDTPA-loaded poly(lactic-*co*-glycolic acid) (PLGA) NPs,[15] or for GdCAs entrapped in the inner-core of liposomes.[16] This may indicate that in vivo the hydrogel nature of GdDOTA⊂NPs is efficient at preventing rapid $[GdDOTA]^-$ leakage, even without covalent linkage of the GdCAs to the polymer matrix.

Nanoparticle relaxivities were measured at 37 °C and 60 MHz (1.5 T). On a per millimolar Gd basis, the particles presented an r_1 of 72.3 $s^{-1}mM^{-1}$ and an r_2 of 177.5 $s^{-1}mM^{-1}$ (i.e. 24 times higher for r_1 and 52 times higher for r_2 at 60 MHz compared to the free complex). The resulting relaxivity values were similar to those of Gd-loaded liposomes[15] or compartmentalized gadolinium complexes in the apoferritin cavity.[16] It is also worth noting that the measured relaxivity values at 300 MHz (approximately 9.5 $s^{-1}mM^{-1}$ at 37 °C) are still remarkable for biological applications as a high-field CA.

The longitudinal relaxation rates were then recorded at 37 °C as a function of resonance frequency and according to NP Gd-loading (Supporting Information, Figure S5). The corresponding NMR dispersion (NMRD) profiles (Figure 2) were characterized by a maximum in relaxivity between 25 and 30 MHz.

This result indicates that inside the hydrogel, GdCA rotational motion is restricted.[17] It can be estimated through the high-field dispersion that τ_R is in the nanosecond range, where τ_R is the rotational correlation time which describes the rotational motion of the complex. Furthermore relaxivity slightly decreased with decreasing temperature (Supporting Information, Table S4), indicating a slow exchange regime for the exchangeable inner-sphere water molecule of GdDOTA. The very large relaxivity obtained at 25–30 MHz could suggest a strong outer-sphere and/or second-sphere contribution to the relaxivity. This hypothesis is supported by the fact

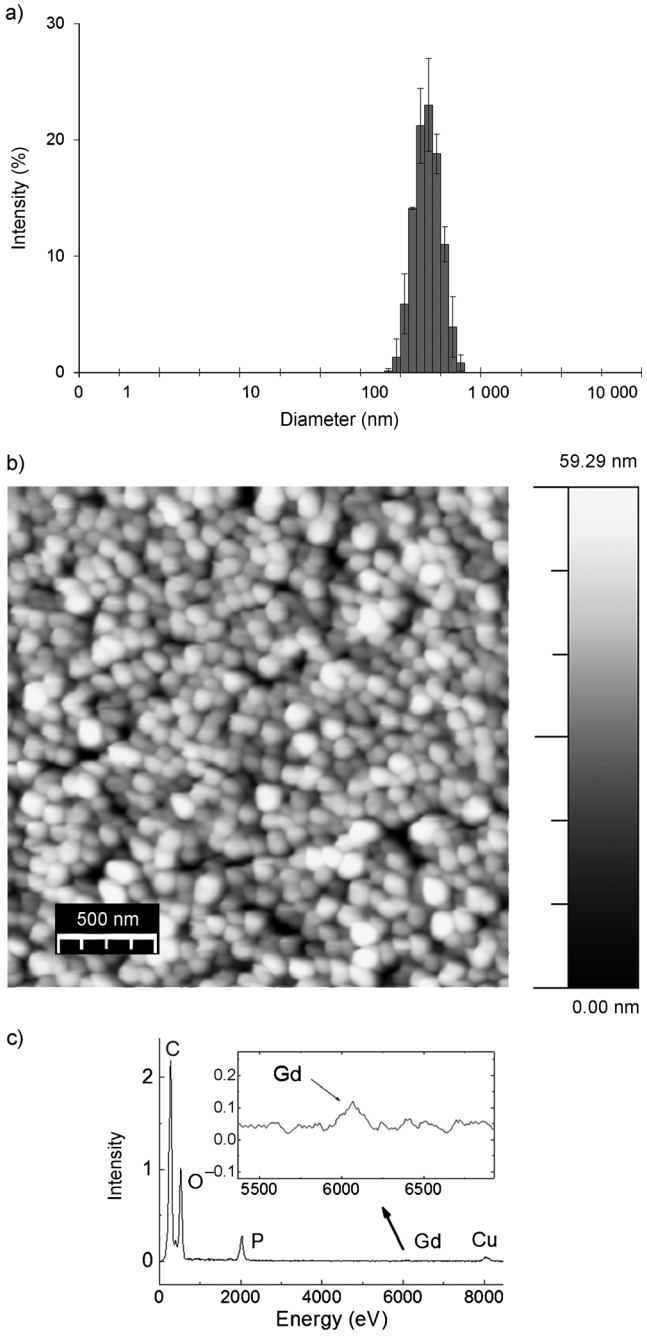

Figure 1. a) DLS spectrum for GdDOTA⊂NPs; b) corresponding AFM image; c) TEM-EDXS on the same sample showing a characteristic Gd signal.

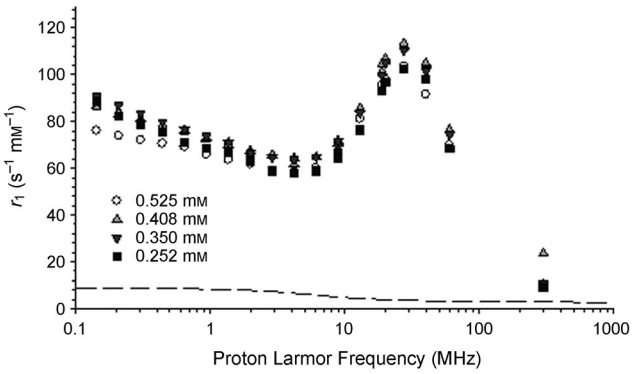

Figure 2. NMRD relaxivity profiles of GdDOTA⊂NPs at various concentrations (dotted line = H[GdDOTA]) at 37 °C.

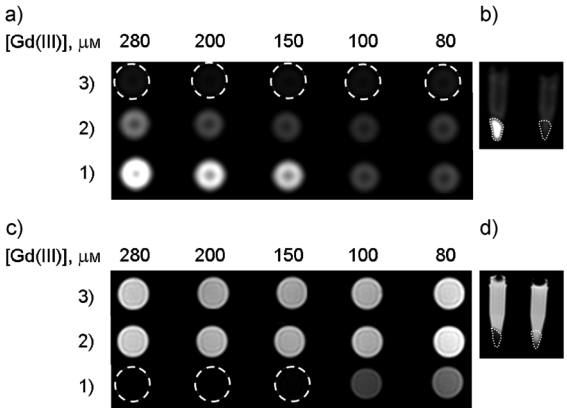

Figure 3. a) T_1-weighted images of 1) GdDOTA⊂NPs, 2) DOTAREM, and 3) water, as a control. b) T_1-weighted MR images of C6 cell pellets incubated with 50 μM of either DOTAREM (right) or 50 μM GdDOTA⊂NPs (left) for 1×10^6 cells in 1.5 mL of PBS. c) T_2-weighted images for the same solutions as in (a). d) T_2-weighted MR images of the same C6 cell pellets as in (b). All samples imaged at 3 T, 37 °C, and standard spin echo (SE) sequence.

that both CH and HA are highly hydrophilic[18] and provide a favorable aqueous environment for GdCAs.

To demonstrate how this relaxation enhancement was translated into contrast, T_1- and T_2-weighted images of phantoms containing suspensions of GdDOTA⊂NPs were acquired on a 3 T clinical imager, with DOTAREM as a control (Figure 3 a,c). For the T_1-weighted images, the bright signal enhancement progressively increased with increased GdDOTA⊂NP concentration. For the T_2-weighted images, under the same concentration conditions, image darkening was observed with the increase of GdDOTA⊂NP concentration. Comparison with the controls showed that the enhanced signals (positive or negative) were inherent only to GdDOTA⊂NPs. These images corroborated the relaxometric results and highlighted the dual properties of the present nanoparticles. This GdDOTA⊂NP behavior could be interpreted by 1) the occurrence of entrapped GdCAs in a highly hydrated pocket, as shown by the large r_1 values and 2) an important T_2 effect at high magnetic-field strength. This large T_2 resulted from the slow rotation of the Gd-complex but magnetic-susceptibility effects caused by magnetic-field gradients induced by the difference in magnetic susceptibility between the inner- and outer-nanoparticle environment could also contribute, as already reported for liposomal systems.[16,19] This second phenomenon still remains to be investigated.

Thus, the hydrogel structure of the matrix greatly amplified the magnetic properties of the encapsulated $[GdDOTA]^-$. From an imaging point of view, this result is very interesting because without drastic synthetic modifica-

tions to the Gd chelate, it was possible to magnify its MRI properties and to combine strong T_1- and T_2-contrast effects in a single nanoparticle.[20]

Finally, cell viability was monitored using an MTT assay to measure the mitochondrial enzyme activity of C6 glioma cells (Supporting Information, Figure S6). The results of the assay showed that GdDOTA⊂NPs were not toxic to these cells; they were viable even after incubation with a nanoparticle loading of 23 $\mu g\,mL^{-1}$ per 5×10^4 C6 cells for 48 hours. Furthermore, as shown in Figure 3b,d, for the C6 cells pre-incubated for 2.5 hours with 50 μM GdDOTA⊂NPs, significant signal enhancements were measured both in T_1- and T_2-weighted images. After the cell pellets were imaged, they were digested under acidic conditions and the amount of Gd taken up by the C6 cells during incubation was determined by ICP-AES to be 7.9 % of the initial Gd amount (approximately 300 NPs per cell). Thus, the combination of intrinsic enhanced NP relaxivity with an intracellular NP accumulation led to an exacerbated MRI signal enhancement, even for a low Gd concentration.

In conclusion, a spectacular boost in relaxation rate was found in GdDOTA-loaded polymeric nanoparticles, GdDOTA⊂NPs. This valuable enhancement could partially originate from the hydrogel matrix structure and from the efficient and stable loading of Gd. Therefore, these new nanoparticles turn a widely-used and safe CA, that is, DOTAREM, into a powerful T_1/T_2 dual-mode contrast agent. Currently, the routine diagnostic approach of perfusion is based on the assessment of enhanced T_1-weighted MR images. Obtaining both T_1- and T_2-weighted gadolinium-enhanced MR images may offer new possibilities for radiologists in terms of evaluation of the perfusion of a specific organ and for disease characterization. The new synthetic approach developed herein has the advantage of producing efficient, biocompatible, bimodal contrast agents using a straightforward and easily scalable process.

Received: April 25, 2012
Revised: June 2, 2012
Published online: August 2, 2012

Keywords: T_1/T_2 contrast agents · gadolinium · gels · imaging agents · nanoparticles

[1] a) E. Toth, L. Helm, A. E. Merbach, *The Chemistry of Contrast Agents in Magnetic Resonance Imaging* (Eds.: A. E. Merbach, E. Toth), Wiley, Chichester, **2001**, pp. 45 – 119; b) P. Hermann, J. Kotek, V. Kubíček, I. Lukeš, *Dalton Trans.* **2008**, 3027 – 3047.
[2] M. Port, J. M. Idée, C. Medina, C. Robic, M. Sabatou, C. Corot, *BioMetals* **2008**, *21*, 469 – 490.
[3] a) T. Grobner, *Nephrol. Dial. Transplant.* **2006**, *21*, 1104 – 1108; b) J. M. Idée, M. Port, C. Medina, E. Lancelot, E. Fayoux, S. Ballet, C. Corot, *Toxicology* **2008**, *248*, 77 – 88.
[4] N. Bloembergen, L. O. Morgan, *J. Chem. Phys.* **1961**, *34*, 842 – 850.
[5] a) P. Caravan, *Chem. Soc. Rev.* **2006**, *35*, 512 – 523; b) E. Terreno, D. Delli Castelli, A. Viale, S. Aime, *Chem. Rev.* **2010**, *110*, 3019 – 3042.
[6] M. Botta, L. Tei, *Eur. J. Inorg. Chem.* **2012**, 1945 – 1960.
[7] J. Della Rocca, W. Lin, *Eur. J. Inorg. Chem.* **2010**, 3725 – 3734.
[8] B. Sitharaman, K. R. Kissell, K. B. Hartman, L. A. Tran, A. Baikalov, I. Rusakova, Y. Sun, H. A. Khant, S. J. Ludtke, W. Chiu, W. Laus, E. Toth, L. Helm, A. E. Merbach, L. J. Wilson, *Chem. Commun.* **2005**, 3915 – 3917.
[9] a) H. B. Na, T. Hyeon, *J. Mater. Chem.* **2009**, *19*, 6267 – 6273; b) C. Alric, J. Taleb, G. Le Duc, C. Mandon, C. Billotey, A. Le Meur-Herland, T. Brochard, F. Vocanson, M. Janier, P. Perriat, S. Roux, O. Tillement, *J. Am. Chem. Soc.* **2008**, *130*, 5908 – 5915; c) L. Moriggi, C. Cannizzo, E. Dumas, C. R. Mayer, A. Ulianov, L. Helm, *J. Am. Chem. Soc.* **2009**, *131*, 10828 – 10829; d) J. S. Ananta, B. Godin, R. Sethi, L. Moriggi, X. Liu, R. E. Serda, R. Krishnamurthy, R. Muthupillai, R. D. Bolskar, L. Helm, M. Ferrari, L. J. Wilson, P. Decuzzi, *Nat. Nanotechnol.* **2010**, *5*, 815 – 821; e) M. F. Ferreira, B. Mousavi, P. M. Ferreira, C. Martins, L. Helm, J. A. Martins, C. F. G. C. Geraldes, *Dalton Trans.* **2012**, *41*, 5472 – 5475.
[10] M. Dasha, F. Chiellini, R. M. Ottenbriteb, E. Chiellini, *Prog. Polym. Sci.* **2011**, *36*, 981 – 1014.
[11] F. A. Oyarzun-Ampuero, J. Brea, M. I. Loza, D. Torres, M. J. Alonso, *Int. J. Pharm.* **2009**, *381*, 122 – 129.
[12] Optimization of the nanoparticle synthesis with respect to the CH/HA ratio and the nature of the contrast agent is reported in the Supporting Information.
[13] E. Battistini, E. Gianolio, R. Gref, P. Couvreur, S. Fuzerova, M. Othman, S. Aime, B. Badet, P. Durand, *Chem. Eur. J.* **2008**, *14*, 4551 – 4561.
[14] S. A. Agnihotri, N. N. Mallikarjuna, T. M. Aminabhavi, *J. Controlled Release* **2004**, *100*, 5 – 28.
[15] A. Doiron, K. Chu, A. Ali, L. Brannon-Peppas, *Proc. Natl. Acad. Sci. USA* **2008**, *105*, 17232 – 17237.
[16] S. Aime, D. Delli Castelli, D. Lawson, E. Terreno, *J. Am. Chem. Soc.* **2007**, *129*, 2430 – 2431.
[17] S. Aime, L. Frullano, S. Geninatti Crich, *Angew. Chem.* **2002**, *114*, 1059 – 1061; *Angew. Chem. Int. Ed.* **2002**, *41*, 1017 – 1019.
[18] J. A. Burdick, G. D. Prestwich, *Adv. Mater.* **2011**, *23*, H41 – H56.
[19] S. L. Fossheim, A. K. Fahlvik, J. Klaveness, R. N. Muller, *Magn. Reson. Imaging* **1999**, *17*, 83 – 89.
[20] D. Yoo, J. H. Lee, T. H. Shin, J. Cheon, *Acc. Chem. Res.* **2011**, *44*, 863 – 874.

